Responses to Reviewers' Comments on Manuscript egusphere-2024-3666

Machine Learning Assisted Inference of the Particle Charge Fraction and the Ion-induced Nucleation Rates during New Particle Formation Events

We are grateful for the comments from the reviewers which have helped us further improve the manuscript. Please find our point-to-point responses below. The line numbers refer to the revised manuscript without tracked changes. Comments from the reviewers start with '•' and the revised texts are shown in blue.

Reviewer: 1

General comment

- Authors implemented their previously developed numerical model to simulate the dynamics of charge fraction during NPF events. They also implemented machine learning algorithms to expediate their simulation. Forward simulation outputs the charge fraction as a function of particle diameter, and the reverse simulation outputs the fraction of ion-induced nucleation (IIN) from given set of charge fraction vs size. Authors systematically analyzed how each input parameters of NPF (e.g, GR, N_{ion}, J_{IIN}, CoagS) affects the size dependence of charge fraction over 3-20 nm particle diameter range. It was also surprising to see that charge fraction goes below steady state value when the recombination among charged particles was included, and I hope that authors will have opportunities in their future to prove the observed tend with those measured during atmospheric aerosol sampling. Authors have shown the conditions in which the reverse simulation can estimate the value of F_{INN}, and indicated that the charge fraction at smallest measurable size is needed to predict F_{INN}. Authors also showed that the sensitivity of the reserve calculation is influenced by the criteria used to select training data. My comment is positive, and I recommend the publication of this study in ACP after some minor corrections are made.

Specific comments

- The left-hand side of Equation 1 should be the rate expression.

Reply: We thank the reviewer for catching this mistake. The left-hand side of Eq. 1 has been changed to $\frac{dn_{d_p,k}}{dt}$.

- Line 276 to Line 277: I think that how far from the initial charge state to the steady state value also affect the value of tao.

Reply: This is an excellent point. A rearrangement of Eq. S10 leads to

$$\left|\frac{N_1(t)}{N_{1,ss}}-1\right| = \left|\frac{N_1(0)-N_{1,ss}}{N_{1,ss}}\right| \exp\left(-(2\beta_0+\beta_1)\frac{N_{ion}}{2}t\right) = \left|\frac{f_1(0)-f_{1,ss}}{f_{1,ss}}\right| \exp\left(-(2\beta_0+\beta_1)\frac{N_{ion}}{2}t\right) \quad \text{(R1)}$$

where $f_1(0)$ is the initial singly charged fraction and $f_{1,ss}$ is the steady-state singly charged fraction. The distance between the two fractions, i.e., $|f_1(0)-f_{1,ss}|$ apparently affects τ_{ss}. To make this clear we made the following revisions:

Revised SI, line 70:

The solution of Eq. (S9) is

$$N_1(t) = \frac{\beta_0 N_t}{2\beta_0+\beta_1}\left(1-\exp\left(-(2\beta_0+\beta_1)\frac{N_{ion}}{2}t\right)\right) + N_1(0)\exp\left(-(2\beta_0+\beta_1)\frac{N_{ion}}{2}t\right) \quad \text{(S10)}$$

According to Eq. (S10), the steady-state N_1 value is $N_{1,ss} = \frac{\beta_0 N_t}{2\beta_0+\beta_1}$. Rearranging Eq. (S10) leads to

$$\left|\frac{N_1(t)}{N_{1,ss}}-1\right| = \left|\frac{N_1(0)-N_{1,ss}}{N_{1,ss}}\right| \exp\left(-(2\beta_0+\beta_1)\frac{N_{ion}}{2}t\right) = \left|\frac{f_1(0)-f_{1,ss}}{f_{1,ss}}\right| \exp\left(-(2\beta_0+\beta_1)\frac{N_{ion}}{2}t\right) \quad \text{(S11)}$$

where $f_1(0) = \frac{N_1(0)}{N_t}$ and $f_{1,ss} = \frac{N_{1,ss}}{N_t}$ are the fractions of singly charged particles (of one polarity) at t=0 and at steady state, respectively. This equation shows the difference between the initial and steady state charge fraction, i.e.,$|f_1(0)-f_{1,ss}|$, decays exponentially with time. For the two extreme cases we consider, Eq. (S11) leads to

$$\begin{cases} 1-\frac{f_1(t)}{f_{1,ss}} = \exp\left(-(2\beta_0+\beta_1)\frac{N_{ion}}{2}t\right), & \text{if } f_1(0)=0 \\ \frac{f_1(t)}{f_{1,ss}}-1 = \frac{\beta_1}{2\beta_0}\exp\left(-(2\beta_0+\beta_1)\frac{N_{ion}}{2}t\right), & if\ f_1(0)=\frac{1}{2} \end{cases} \quad \text{(S12a, b)}$$

Equations S12a and S12b correspond to initially neutral and charged particles, respectively. According to our definition (see main text) of the characteristic time τ_{ss}, setting the left-hand side of Eq. S12 to 1/e leads to the expression for τ_{ss}:

$$\tau_{ss} = \begin{cases} \frac{2}{(2\beta_0+\beta_1)N_{ion}}, & \text{if } f_1(0)=0 \\ \frac{2+2\ln\left(\frac{\beta_1}{2\beta_0}\right)}{(2\beta_0+\beta_1)N_{ion}}, & \text{if } f_1(0)=\frac{1}{2} \end{cases} \quad \text{(S12a, b)}$$

Revised manuscript, line 288: Theoretical analysis (Sect. S3 in the SI) shows that τ_{ss} can be

expressed as:

$$\tau_{ss} = \begin{cases} \frac{2}{(2\beta_0+\beta_1)N_{ion}}, & \text{if } f_1(0) = 0 \\ \frac{2+2\ln\left(\frac{\beta_1}{2\beta_0}\right)}{(2\beta_0+\beta_1)N_{ion}}, & \text{if } f_1(0) = \frac{1}{2} \end{cases} \quad (13)$$

where $f_1(0)$ is the initial fraction of singly charged particles (of one polarity). Apparently, for particles of all sizes, τ_{ss} is inversely proportional to the ion concentration. Additionally, at a fixed ion concentration, τ_{ss} stays relatively constant or decreases with increasing particle size. This trend is caused by the variation of the collision rate constants $(2\beta_0 + \beta_1)$ as particle size increases, to which τ_{ss} is also inversely proportional (Eq. (13)). Further comparison between Fig. 2a and Fig. 2b reveals that τ_{ss} is smaller for initially neutral particles than initially fully charged particles. As demonstrated in the SI, the characteristic time depends on $|f_1(0) - f_{1,ss}|$, i.e., the distance between the initial and steady state singly charge fraction. This distance is larger for initially charged particle and results in an extra term $\ln\left(\frac{\beta_1}{2\beta_0}\right)$ in Eq. (13).

- In the paragraph between Line 268 to Line 277, the statements refer to Equation S12 multiple times. It helps readers to be able to see Equation S12 in the main article.

Reply: This is a good advice. We have relocated the original Eq. S12 to the main text to help the reader to better understand the text. Please refer to our response to the previous comment.

- In the paragraph named "Section 3.3 ResNet Assisted inference of F_{IIN}". It is recommended that author provide additional explanation about why and how the difference in the value of the Greek letter "Chi" affects the sensitivity S_x.

Reply: We thank the reviewer for the suggestion. We acknowledge the importance of clarifying the influence of χ on the sensitivity S_x. Therefore, we made the following revisions:

Revised manuscript, line 463: As particles grow, the information of their initial charge fraction can be obscured by particle-ion interactions. This is demonstrated by the r_c-d_p curves in Figure S8a, which shows that despite the different F_{IIN} (from 0% to 20%), the particle charge fraction already converges to the steady state value (i.e., $r_c = 1$) at $d_p = 2.2$ nm at a high ion concentration ($N_{ion} = 5000$ cm^{-3}). In this case, it becomes impossible to infer F_{IIN} from the observed particle charge state since the r_c-d_p curves are non-distinguishable. In contrast, at a lower ion concentration ($N_{ion} = 450$ cm^{-3}), the r_c-d_p values are still well separated at 2.2 nm (Figure S8b), hence one can deduce F_{IIN} from r_c in this case. In general, for closely spaced r_c-d_p curves at 2.2 nm, the neural network would find it difficult to utilize their difference to infer F_{IIN}. With these considerations, we define a parameter χ as the change of particle charge fraction at 2.2 nm when F_{IIN} changes by 1%, which essentially characterizes the amount of information (regarding F_{IIN})

that are still retained as the particle grow to 2.2 nm The larger χ is, the further apart the r_c-d_p curves are, and the more accurately the neural network can infer F_{IIN}.

Revised manuscript, line 485: In other words, when the r_c-d_p curves (see Fig. S8 for such curves) are closely spaced, a small variation of r_c may correspond to a large variation of F_{IIN}.

Revised SI, Fig. S8:

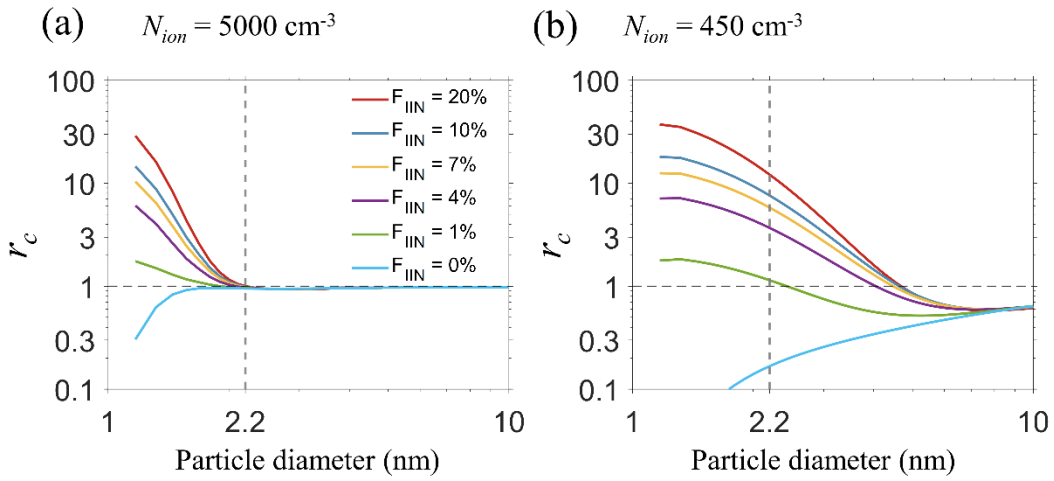

Figure S8. r_c as a function of particle diameter at different ion concentrations (a) N_{ion} = 5000 cm^{-3}; (b) N_{ion} = 450 cm^{-3}. The other simulation conditions are GR = 4 nm h^{-1}, CoagS = 0.005 s^{-1}, J = 100 cm^{-3} s^{-1}.

Minor comments

- L164: “additional” => “addition”
- L225: “Neutral” => “Neural”
- L372: “Resnet” => “ResNet”

Reply: The typos has been corrected.

Reviewer: 2

- The authors present a numerical model to simulate the charging dynamics of newly formed aerosol particles. They use machine learning to infer the fraction of ion-induced nucleation. The model is valuable and the paper is interesting and likely useful. The language is generally clear and the paper is well-written and well-referenced with useful supplementary material. The explanation of the machine learning approach and its results is good. Despite this I found some details of the model description missing and some aspects difficult to understand, and recommend the following revisions to help put the model and its results in context.

Major comments

- How is water handled in the model? In dry versus humid environments, how will the microphysical process rates differ?

Reply: We thank the reviewer for the comment. The influence of water is not considered in the current simulation.

There are primarily two mechanisms through which water affects particle charging dynamics: (1) hygroscopic growth changes the particle size and increases the apparent particle growth rate, (2) variation of RH may change the ion properties. To include the first mechanism into the model, one can potentially use a simplified thermodynamics model such as the ZSR rule to calculate the particle size at humid conditions, and then use this 'wet' size in simulation. Unfortunately, there is still a lot we don't know about the hygroscopicity of atmospheric new particles, which is subject to a strong Kelvin effect and the influence of complex particle composition. Therefore, reliable modelling of the hygroscopic growth of new particle is currently out of reach. However, our simulation offers some qualitative evidence into how hygroscopic may change the charging dynamics: Compared to the dry conditions, water uptake by particles increase their apparent growth rate. As a result, considering particle hygroscopic growth roughly corresponds to simulation results at a higher GR.

As to the second mechanism, a few studies have shown that both the ion mobility and composition are influenced by humidity (Oberreit et al., 2015; Liu et al., 2020; Luts et al., 2011). The clustering of water with ions may decrease the ion mobility and reduce the ion-particle collision rates. However, the influence of RH on ion mobility is difficult to quantify based on the existing literature, hence we did not consider this in the manuscript.

We added further notes to the revised manuscript:

Revised manuscript, line 89: Although particles may absorb ambient water vapor, we do not include particle hygroscopic growth in the simulation. Subject to the influence of a strong Kelvin effect and a complex chemical composition, the hygroscopic growth factor of atmospheric new particles has high uncertainties. Despite this neglect, water uptake may lead

to increased particle growth rates in simulations compared to dry particles. The effect of higher particle growth rates on particle charging dynamics is examined thoroughly in the following.

Revised manuscript, line 203: A few studies have also shown that both the ion mobility and ion composition are influenced by humidity (Oberreit et al., 2015; Liu et al., 2020; Luts et al., 2011). The clustering of water with ions may decrease the ion mobility and reduce the ion-particle collision rates. However, such effect is difficult to quantify based on existing research, hence in the simulation we did not consider ion hydration.

- What were the conditions for the simulations shown in Figure 2? Does this figure represent a large number of calculations performed with monodisperse size distributions?

Reply: Yes, this figure represents a large number of calculations performed with monodisperse particles. To make the simulation conditions clear, we made the following revisions:

Revised manuscript, line 271: To estimate the time scale for particles to achieve steady-state charge distribution under different ion concentrations, we numerically solved Eq. (1) to simulate the charge state evolution of monodisperse particles in the size range of 1-100 nm. The ion properties are listed in Table 1 and the simulation was conducted at a temperature of 298.15 K at atmospheric pressure. Below we discuss two extreme cases: initially neutral and initially fully charged particles (50% positively charged, 50% negatively charged). These cases correspond to the maximum timescale to reach the steady state from two different directions, while other scenarios in between would have shorter timescales.

- Figure 3 and Figure 4: I found this ratio r_c hard to interpret. It would be helpful to add a right-hand y axis to all of these figures to show how the absolute value of the steady-state singly charged fraction varies with the variable plotted on the x axis. Generally through the paper, I found it hard to get a feeling for this pervasive r_c ratio without knowing what the steady-state charge distribution actually is.

Reply: We agree it would be better to add the steady state value to Figures 3 and 4. For Figure 3, because we only examine a few particle size ranges, we added the steady state charge fraction of the median size particles in each range to the figure caption. In Figure 4, we added the absolute value of the steady-state singly charged fraction to the figures.

Revised manuscript, line 323: The red, black, blue, and yellow curves represent four different particle size ranges (shown in the figure legend), with steady-state singly charged fractions of 0.0168, 0.0483, 0.0931 and 0.1975, respectively. These values are evaluated at the median of each size range, i.e., 3.5 nm, 7 nm, 11 nm and 20 nm. The absolute charge fraction of the particles can be obtained by multiplying r_c by the corresponding steady-state charge fraction.

Revised manuscript, figure 4:

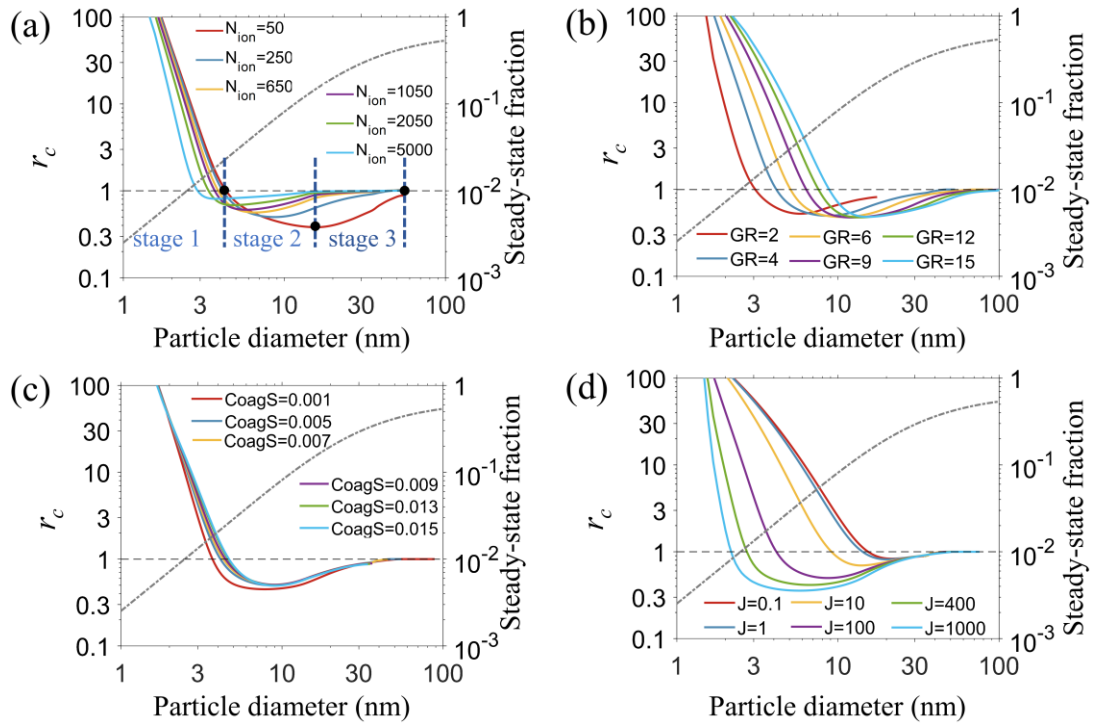

Revised manuscript, line 366: The units for N_{ion}, GR, CoagS, and J in the figure legends are cm^{-3}, nm h^{-1}, s^{-1} and cm^{-3} s^{-1}, respectively. For reference, the steady-state singly charged fractions of particles are also plotted as a function of size (dash-dot lines, right y axis). The absolute singly charged fraction of the particles can be obtained by multiplying r_c by the steady-state charge fraction.

- It would be beneficial to put the results into the context of the dynamics of the atmospheric ions. During a nucleation event, ion concentrations are likely to decrease. This is not simulated, but it would be helpful if the authors could describe the scale of the changes expected during a realistic NPF event and relate them to the changes they are studying here. Also, a lot of the timescales are very long compared to other expected changes.

Reply: This is a good advice. Yes, the atmospheric ion concentration constantly changes due to varying production and loss rates, and in many reported cases NPF concurs with a decrease in ion concentration. Some field observations have tracked the concentration variation of atmospheric ions during NPF. These data, along with our sensitivity analysis, helps us to give a rough estimate of the uncertainties regarding the particle charge fraction:

Revised manuscript, line 439: Despite good agreement with the benchmark model, the applicability of the ResFWD is limited by the data used for its training. For instance, we have assumed constant ion concentration during NPF, which in reality changes due to varying ion production and loss rates in the atmosphere. Observations suggest that NPF often concurs with a decrease in the concentration of small ions, and the extent of decrease varies between different field campaigns. (Note that for continental stations, the ion concentration usually has the

highest value in the morning and lowest value in the afternoon, possibly due to the variation of radon concentration (Hõrrak et al., 2003). This decreasing trend of ion concentration proceeds simultaneously with many NPF events.) Data from the Tahkuse Observatory in the warm season of 1994 show that the concentration of small cluster ions (mobility between 1.3–3.14 $cm^2 V^{-1} s^{-1}$) decreased by approximately 20% from 8:00 to 12:00 (Horrak et al., 2003). Huang et al. (2022) shows that the concentration the ions (mobility between 0.5–3.14 $cm^2 V^{-1} s^{-1}$) decreases less than 25% within during NPF events. Recently, Zhang reported that the median of ion concentration (mobility between 0.5–3.14 $cm^2 V^{-1} s^{-1}$) decreased by less than 10% from 9:00 and 15:00 during event days at the SMEAR II station, and less than 25% at the SORPES station.

According to the field observations, it is reasonable to assume that in a typical NPF event, the ion concentration vary by $\pm$10% around its mean value. Based on our sensitivity analysis (Fig. 5f), a $\pm$10% variation of N_{ion} leads to an uncertainty of F_{IIN} mostly by less than $\pm$20%. However, to develop a rigorous quantitative relation between input variation and the particle charge fraction, further simulations with time varing inputs are needed. Additionally, we did not consider scenarios where the mobilities and concentrations of atmospheric positive and negative ions differ, restricting the direct application of ResFWD in these cases. The applicability of ResFWD can be further expanded by training the neural network with a larger dataset that includes the above considerations.

- The authors should make their model code public or explain why they cannot do so and provide the code to the reviewers as described here: https://www.atmospheric-chemistry-and-physics.net/policies/data_policy.html. Also, the authors should comply with "The data needed to replicate figures in a paper should in any case be publicly available".

Reply: We have uploaded all the data needed to reproduce the figures to Zenodo. The DOI is https://doi.org/10.5281/zenodo.15024817.

Although we have a plan to make the code public, there are certain code functionalities which require further work. Additionally, a user-friendly interface and a complete manual are yet to be finished. Therefore, we have uploaded the code with which we performed the current studies so that it can be inspected by the reviewer.

Revised manuscript, line 520: All the data needed to reproduce the figures can be found at https://doi.org/10.5281/zenodo.15024817.

Minor comments

- L53 Recent papers by Mahfouz and Donahue are relevant here

Reply: We have added Mahfouz and Donahue (2021) as a reference.

- L56: INN typo for "IIN"

Reply: The typo has been corrected.

- L104: Eqn 1 does not appear to be dimensionally consistent. It is an ion balance of sources and sinks. Presumably there is some multiplication by time step or derivative missing. The similar equations in the supplement make more sense.

Reply: The left-hand side of Eq. (1) has been changed to $\frac{dn_{d_p,k}}{dt}$.

- L110 please explain where in the cited Lopez-Yglesias and Flagan paper equation 2 comes from, or otherwise explain how it was determined. Also specify dimensions (units) of beta values.

Reply: Equation 2 is presented in the supplemental information of Yglesias and Flagan (2013). This information along with variable dimensions has been added to the revised manuscript.

Revised manuscript, line 114: In this study, we used the rate coefficients developed by López-Yglesias and Flagan (2013) (see the SI of this work).

Revised manuscript, line 117: …where $\beta_{d_p,k,\pm}$ is in unit of m^3/s, d_p is in unit of meters, $B_{q,\pm}(k)$ are dimensionless fit coefficients, q is number of charges on the particle, and $Q = 23$ is the maximum of q.

- Please use and define consistent expressions for Boltzmann's constant between eq 4 and eq 8

Reply: We have checked the symbol consistency between Eq. (4) and (8). For clarity, we use q to replace k as the number of charges on the particle in the modified equations.

- L121 specify equation number in Gopalakrishnan and Hogan

Reply: The equation number has been specified.

Revised manuscript, line 126: To calculate β_i in Eq. (3), we first calculated the collision rate coefficients with Eqs. (12) and (14) in Gopalakrishnan and Hogan (2011) and…

- L134 specify what is meant by a Lagrangian approach (or at least specify that the sectional scheme is double-moment, if that is correct)

Reply: We have removed the phrase 'Lagrangian approach' to avoid confusion. Additionally, we make it clear that both the particle number and mass are tracked in each section:

Revised manuscript, line 141: Within each simulation interval (20 s), we calculated the mass change of particles due to condensation/evaporation in each subsection using the approach described in Zaveri et al. (2008). At the end of an interval, the particles are distributed into different mass bins using the Linear Discrete Method (Simmel and Wurzler, 2006). To

implement this method, both the particle number and mass are tracked in each section. The particle charge state was preserved during particle growth.

- It would be helpful to summarize, perhaps in a table, what is held constant in the model-vapor concentrations, ion concentrations, perhaps? What are the implications of this for how realistic the results are?

Reply: This is a good suggestion. To make it clear what quantities are held constant during the simulation, we have added a note to Table 1.

In some NPF events, key variables such as GR, N_{ion} are indeed close to constants with small variations. In these cases, how small variations of GR and N_{ion} affect particle charge states can be inferred from the sensitivity analysis such as Figure 5. However, a rigorous, more general analysis of how strongly varying GR and N_{ion} affect our results requires further work. This point is made clear in the last two sentences of the manuscript.

Revised manuscript, line 224: *All parameters except GR are explicitly held constant in a simulation. GR is determined from vapor condensation rates (vapor concentrations are held constant) and barely changes with particle size (see Fig. S1b), hence GR can also be regarded as a constant.

- Figure 2: it would be helpful to state how these characteristic times compare to the appropriate recombination lifetime and ion-aerosol attachment lifetimes. Do these mean some of the parameter space shown in the figure is not relevant?

Reply: We thank the reviewer for the comment. Figure 2 is presented to provide readers with a sense of the particle charging time scale at atmospherically-relevant ion concentrations.

Both ion-ion recombination and ion-aerosol attachment consume atmospheric ions. The time scale of these processes is of paramount importance if we are interested in the atmospheric ion concentration. However, since we have treated N_{ion} as an input to our simulation, it could be a bit off-topic to discuss such time scales. Additionally, a reasonable discussion of these time scale must be put in the context of ion production rates in the atmosphere, which is highly variable with respect to locations and time. Based on the above reasons, we have not incorporated discussions on ion- ion recombination lifetime and ion-aerosol attachment lifetime in the revised manuscript.

- L331 lt is not clear to me that this statement would be true at the very high ion concentrations produced by a typical ion source in an SMPs, e.g. Polonium. What ion concentrations are realistic for an SMPS?

Reply: The statement is only true at atmospheric ion concentrations. In an ion source, the characteristic time to reach steady state charge distribution is much shorter due to the high ion

concentration, which is typically on the order of 10^6-10^7 cm^{-3} (Liu and Pui, 1974; Liu et al., 1986).

Revised manuscript, line 354: Our analysis demonstrates that during NPF events, freshly formed neutral particles require tens of minutes to hours to achieve this steady-state distribution through interaction with atmospheric ions.

- Conclusion: perhaps let other researchers determine whether or not the study is "pioneering"

Reply: The word "pioneering" has been replaced by “initial”.

References:

Liu, B. Y. H. and Pui, D. Y. H.: Electrical neutralization of aerosols, J. Aerosol Sci, 5, 465-472, https://doi.org/10.1016/0021-8502(74)90086-X, 1974.

Liu, B. Y. H., Pui, D. Y. H., and Lin, B. Y.: Aerosol Charge Neutralization by a Radioactive Alpha Source, Particle & Particle Systems Characterization, 3, 111-116, https://doi.org/10.1002/ppsc.19860030304, 1986.

Liu, Y., Attoui, M., Yang, K., Chen, J., Li, Q., and Wang, L.: Size-resolved chemical composition analysis of ions produced by a commercial soft X-ray aerosol neutralizer, J. Aerosol Sci, 147, 105586, https://doi.org/10.1016/j.jaerosci.2020.105586, 2020.

Luts, A., Parts, T.-E., Hõrrak, U., Junninen, H., and Kulmala, M.: Composition of negative air ions as a function of ion age and selected trace gases: Mass- and mobility distribution, J. Aerosol Sci, 42, 820-838, https://doi.org/10.1016/j.jaerosci.2011.07.007, 2011.

Mahfouz, N. G. A. and Donahue, N. M.: Atmospheric Nanoparticle Survivability Reduction Due to Charge-Induced Coagulation Scavenging Enhancement, Geophys. Res. Lett., 48, e2021GL092758, https://doi.org/10.1029/2021GL092758, 2021.

Oberreit, D., Rawat, V. K., Larriba-Andaluz, C., Ouyang, H., McMurry, P. H., and Hogan, C. J., Jr.: Analysis of heterogeneous water vapor uptake by metal iodide cluster ions via differential mobility analysis-mass spectrometry, J. Chem. Phys., 143, 104204, 10.1063/1.4930278, 2015.